Journal of Translational Medicine

RESEARCH

Open Access

Pharmacological Vitamin C-induced high H_2O_2 generation mediates apoptotic cell death by caspase 3/7 activation in breast cancer tumor spheroids

Ali Mussa[1,2], Mahasin Hamid[3,4], Khalid Hajissa[5,13], Ahmad Hafiz Murtadha[6], Mohammad A. I. Al-Hatamleh[7], Noor Fatmawati Mokhtar[6,12], Vuk Uskoković[8,9], Magdalena Plebanski[10], Rohimah Mohamud[11*] and Rosline Hassan[1*]

Abstract

Background Pharmacological vitamin C (Vit-C), or high-dose Vit-C has recently gained attention as a potential cancer therapeutic. However, the anticancer activity of Vit-C has not been investigated in realistic 3D models of human cancers, especially with respect to breast cancer (BC), and its potential benefits remain under debate. Herein, we investigate the activity and mechanism of action of pharmacological Vit-C on two BC tumor spheroids.

Methods We developed two distinct types of BC tumor spheroids from MDA-MB-231 and MCF-7 cells. The spheroids underwent treatment with a range of concentrations of pharmacological Vit-C (1, 5, 10, 15, and 20 mM). Assessments were conducted to determine the cell viability, H_2O_2 levels, glutathione-to-glutathione disulfide (GSH/GSSG) ratios, and apoptosis. Both flow cytometry analyses of Annexin V/PI staining and caspase3/7 activity assay were used to check apoptosis.

Results We showed that Vit-C induced dose-dependent cell death in both types of tumor spheroids, primarily driven by elevated H_2O_2 production and a concomitant oxidative stress imbalance induced by the GSH depletion. The high levels of H_2O_2 generated by Vit-C triggered the apoptosis of spheroids. In MCF-7 spheroids, Vit-C-induced H_2O_2 production was higher, with a more pronounced decrease in the GSH/GSSG ratio, indicating greater susceptibility to oxidative stress-induced cell death. However, MDA-MB-231 spheroids exhibited a more severe cytotoxic response.

Conclusions This study reveals that Vit-C induces oxidative stress-mediated cell death in both non-aggressive and aggressive BC spheroids. Unlike traditional in vitro studies, this work provides novel insights into the response of two BC tumor subtypes to Vit-C, demonstrating its potential as a targeted common therapy for BC.

Keywords Vitamin C, Pharmacology, Oncology, Spheroids, Breast cancer, Free radicals

*Correspondence:
Rohimah Mohamud
rohimahm@usm.my
Rosline Hassan
roslin@usm.my
Full list of author information is available at the end of the article

Introduction

Despite the advancements in treatments, breast cancer (BC) remains one of the major causes of mortality among women worldwide [1]. According to the statistical estimates for 2020, there were nearly 2.3 million new incidences of BC, resulting in about 685,000 deaths, accounting for 11.7% of all tumor cases [1]. As of early 2024, BC has recorded 310,720 new cases and 42,250 fatalities [2], indicating the need for urgent new treatment options.

Existing treatments for BC, including immunotherapies, chemotherapies, and radiation, are employed individually or in combination [3, 4]. Either way, they give rise to challenges, including poor targeting and systemic toxicity that can adversely affect multiple organs, like the heart and kidneys. Additionally, these treatments may promote infertility and, in extreme cases, mortality [3, 4]. The presence of such serious adverse effects emphasizes the importance of developing new, safe, and more affordable treatments for BC.

Research on such novel therapeutic options has been hampered by the cellular heterogeneity and diverse signaling pathways in the BC tumor microenvironment (TME) [5]. This fundamental hindrance to the current drugs and drugs in development could result in the initiation, progression and suppression of the immune response, and resistance of the tumor to the drug [5]. Examining the intricate TME is difficult and necessitates the use of sophisticated models, such as 3-dimensional (3D) tumor spheroids. These types of cell culture more accurately mimic the human TME compared to traditional 2-dimentional (2D) culture and animal models [6]. Undoubtedly, 2D cell culture models, alongside animal models, are the fundamental basis for cancer biology research, mostly owing to simplicity, affordability, and ability to be replicated [7]. Nevertheless, 2D cell culture models do not allow the assessment of some of the crucial parameters that govern the TME, including cell–cell contact, hypoxia, cell extracellular matrix (ECM) development, and the flux of nutrients, metabolites and signaling molecules, all of which are fundamental aspects of 3D cell culture models [7], and can dramatically alter drug susceptibility, particularly for drugs that affect metabolic and oxidative pathways, such as Vitamin C (Vit-C). Understanding Vit-C mechanism of action in 3D cultures will be crucial to further optimization. Indeed, tumor spheroids as 3D cell culture models have been extensively used in researching multiple types of tumors, such as non-small cell lung carcinoma [8], ovarian cancer [9], pancreatic cancer [10], colon tumor [11], oral squamous cell carcinoma [12], and BC [13–17]. These models are enabling the development of more effective anticancer treatments [10, 12, 14, 18–20].

Vit-C or ascorbate, a water-soluble nutrient, has been utilized as a viable option to treat various tumors in in vitro models, in vivo models and animal models, as well as in the clinics when delivered at very high pharmacological concentrations, also termed high-dose Vit-C [21]. Vit-C attacks several cancer vulnerabilities, such as ten-eleven translocations (TETs) dysregulation, and acts as an essential co-factor with Fe^{2+} to activate prolyl hydroxylates (PHDs) and factor-inhibiting hypoxia-inducible factor (FIH) to inhibit HIF-1α, in addition to inhibiting NF-κB [21]. Moreover, Vit-C induces cancer cell death through reactive oxygen species——(ROS; hydroxide ion (OH^-), hydrogen peroxide (H_2O_2), hydroxyl radical ($^{\bullet}OH$), and superoxide ($O_2^{\bullet-}$))——mediated apoptosis via the Fenton reaction and the Haber–Weiss reaction, utilizing the labile iron pool (LIP) as a co-factor [21]. Vit-C can disrupt cancer cell metabolism, especially glycolysis, leading to cancer cell death via induced-energy crisis [22]. In fact, Vit-C can exist in two forms following its autoxidation by ROS: ascorbic intermediate radical ($Asc^{\bullet-}$) and dehydroascorbic acid (DHA), which can pass through the cell membrane via the sodium-dependent Vit-C transporter (SVCT) and glucose transporter 1 (GLUT-1), respectively [21, 23]. ROS-mediated Vit-C oxidation into $Asc^{\bullet-}$ and DHA involves the recycling of reduced glutathione (GSH) and the glutathione disulfide (GSSG) by NADPH inside the cell [21, 23]. This process ultimately depletes GSH levels leading to oxidative stress imbalance.

Moreover, although conventional 2D cell cultures have been widely used in cancer research, they do not precisely mimic the intricate TME. As such, the aim of this study was to determine the potency of Vit-C to mediate cytotoxicity in two different types of 3D BC tumor spheroids. Additionally, we sought to explore the molecular mechanisms that may be responsible for Vit-C-induced cytotoxicity in BC spheroid systems.

Material and methods

Cell lines and 2D monolayer culture

Tow cell lines (MDA-MB-231 and MCF-7) were obtained from the ATCC (American Type Culture Collection, USA) and grown in Dulbecco's modified eagle medium (DMEM, Nacalai Tesque, Jaban) supplemented with 5% fetal bovine serum (FBS, Gibco™ (10,270–106) Fetal Bovine Serum; Thermo Fisher Scientific, USA), 2% L-glutamine (Gibco™ L-Glutamine; ThermoScientific, USA), 3 g/500 mL Glucose (G7021-100G) D-(+)-Glucose, Sigma, USA), and 1% penicillin/streptomycin (Gibco™ (10,378–016), Thermo Fisher Scientific, USA). The cells were maintained, passaged until reaching confluency of about 80%, and incubated in 5% CO_2 at 37 °C.

Agarose-coated 96-well plate preparation and 3D spheroids formation

In ultrapure water (50 ml, PURELAB Ultra, UK) a 1.5% agarose (Gibco, USA) was added and autoclaved for 2 min. Then from the solution, 65 µl was placed into each well of the 96-well flat-bottomed plate (Thermo Fisher Scientific, USA) to form a layer of a concave meniscus bottom after solidification, then the 96-well agarose-coated plate was stored in a 4 °C refrigerator until further use. For spheroids generation, following confluency, the cells were trypsinized using Gibco™ Trypsin–EDTA (Gibco, USA) and counted then seeded at a density of 2×10^4 cells/well in the 96-well agarose-coated plate and followed by centrifugation (swing bucket) at room temperature at 1000*g* for 30 min. Then at 37 °C the plates were placed in a 5% CO_2 in the incubator for 3–15 days.

Morphological microscopic assessment

Images of all individual spheroids were taken every two days for 15 days using a camera attached to an inverted fluorescence microscope (Leica Microsystems, Germany) with a 5× objective. All images were analyzed (size and volume) by using the MATLAB-based software SpheroidSizer [24] and ImageJ2 (Fiji) software.

Vit-C preparation and treatment protocol

A stock solution of 200 mM of Vit-C (A7631-100G, Sigma-Aldrich, Germany) was prepared by dissolving 35.224 in 1 ml of ddH_2O, and from the stock solution a working solution in the DMEM media was prepared to have a final 5 doses concentration of Vit-C (1, 5, 10, 15, and 20 mM), as previously stated [25]. After maintaining the spheroids for 3 days, treatment Vit-C designated doses started at day 4, for 72 h in addition to ddH_2O-treated vehicle control (VCTL).

Cell cytotoxicity assay

Following Vit-C treatment, the CellTiter-Glo® 3D Cell Viability Assay (G7571, Promega, USA) was performed at an equal volume of media (100 ul) according to the manufacture protocol, and the luminescence was recorded using the ELISA reader system (SoftMax Pro® 5, Molecular Devices, USA). In another Vit-C-treated groups of spheroids, 300 U/mL of CAT (EC Number: 1.11.1.6, from Bovine Liver; C1345-1G, Sigma-Aldrich, Germany) was introduced to each spheroid/well, and then the same steps of CellTiter-Glo® 3D Cell Viability Assay were applied. VCTL were used to normalize the viability as a percentage. All the experiment were done in the dark.

Cellular ROS detection assay

Following spheroids treatment with different Vit-C doses for 72 h, the cellular ROS was determined by performing the ROS-GLO™ H_2O_2 ASSAY (PROYY-G8820, Promega, USA) according to the protocol from the manufacturer. In short, from the H_2O_2 substrate solution 20 µL was placed to each spheroid/well, and after 6 h incubation at 37 °C in a 5% CO_2 incubator, 100 µL of ROS-GLO™ detection solution (made by mixing 10 mL of luciferin detection reagent with 100 µL of D-Cystein and the signal enhancer solution) was placed together with the H_2O_2 substrate solution and then the mixture incubated for 20–30 min at room temperature, followed by luminescence signal recording using the ELISA reader system (SoftMax Pro® 5, Molecular Devices). Normalization was done to all the experimental data to the control group and conducted all the experiments in the dark.

GSH/GSSG ratio detection assay

The GSH/GSSG-Glo™ Assay (V6611, Promega, USA) was utilized to evaluate the levels of total GSH, oxidized GSSG, and the GSH/GSSG ratio, in accordance with the manufacturer's instructions. In brief, after the treatment with the designated doses of Vit-C to the samples, from the total/oxidized glutathione lysis reagent, 50 µL as well as from the luciferin generation reagent, 50 µL were separately placed in each well containing the spheroids. After shaking the mixture for five minutes, it was allowed to sit at room temperature for thirty min. After that, 100 µL of the luciferin detection reagent was placed in each well, and then the plate was incubated for a further fifteen min. Lastly, the ELISA reader system (SoftMax Pro® 5, Molecular Devices, USA) was used to quantify the luminescence.

Apoptosis detection via annexin V-FITC/PI assay

After 72 h, the spheroids cells were harvested in 15 ml tubes (15 spheroids/tube), then disassociated using Gibco™ Trypsin–EDTA (Gibco, USA). After that, at 1500 rpm the spheroids were centrifuged for 5 min, and 400 µl of trypsin were added to each tube, then transferred to an incubator at 37 °C and CO_2 5 for 20 min. Following this, the cells were resuspended several times in media with a pipette, followed by centrifuging the content at 1500 rpm for 5 min, and the supernatant has been removed and the resultant pellet is ready for apoptosis detection. The Annexin V-FITC/PI Apoptosis Detection Kit (BD, Franklin Lakes, NJ, USA) was used to detect apoptosis. After the spheroids were treated as directed, 100 µL of 1× binding buffer was added to each tube, and the collected cells were incubated with 5 µL of Annexin V-FITC and 5 µL of propidium iodide (PI) for 15 min in

the dark. After that, to the cell tubes, 400 µL of 1 × binding buffer was added, and flow cytometry was utilized to conduct detection using Cell Quest software (BD, SN: E34297502014) (BD, Franklin Lakes, NJ, USA). Following this, the data were processed by FlowJo V10, then normalized against control.

Caspase 3/7 detection

The Caspase-Glo® 3/7 3D Assay (PROYY-G8981, Promega, USA) was utilized in accordance with the manufacturer's protocol to detect apoptosis in control and Vit-C-treated spheroids. This assay contains a luminogenic caspase-3/7 with the tetrapeptide sequence DEVD, a regent optimized for caspase activity, luciferase activity, and cell lysis. In summary, 100 µL of the Caspase-Glo® 3/7 3D reagent was placed in each spheroid/well after the Caspase-Glo® 3/7 3D substrate and thoroughly mixed with it. The mixture was then gently shaken at 500 rpm for about 30 s. The mixture was then incubated at room temperature for 30 min, and the luminescence signal was recorded using an ELISA reader system (SoftMax Pro5®, Molecular Devices, USA). Additionally, every experiment was conducted in the dark and all results were normalized to the control group. Relative caspase 3/7 activity normalized versus control was used to display the data.

Statistical analysis

Statistical analysis was conducted using GraphPad Prism (V 9.1.0, San Diego, CA, USA), and the results are reported as mean ± SEM. The two-tailed unpaired student's *t*-test was applied to statistically comparing two groups, while an ANOVA (one-way analysis of variance) test was utilized for statistical comparison among multiple groups. The statistical significance levels were determined as follows: $^{**}P < 0.01$, $^{***}P < 0.001$, $^{****}P < 0.0001$, and $^{*}P < 0.05$. The significance level for non-significant (ns) results is $P < 0.05$. All the experimental procedures were conducted in triplicates.

Results

The growth kinetics of MDA-MB-231 and MCF-7 tumor spheroids

We utilized two breast cancer cell lines, namely MDA-MB-231 and MCF-7, to create two distinct types of spheroids. The drug resistant, MDA-MB-231 cell line, characterized as invasive ductal carcinoma, exemplifies an aggressive form of triple-negative breast cancer (TNBC) that does not express estrogen receptor (ER), human epidermal growth factor 2 (HER2), or progesterone receptor (PR), categorizing the cells as $HER2^{-}/PR^{-}/ER^{-}$ subtype [26]. The non-metastatic adenocarcinoma MCF-7 cell line, in contrast, represents the less aggressive and non-invasive human breast cancer phenotype that expresses the glucocorticoid receptor, HER2, PR, and the ER [26]. The detailed scheme for the method used to generate the spheroids, involving the seeding of 2×10^4 MDA-MB-231 or MCF-7 cells per well in a 96-well agarose-coated plate, is depicted in Fig. 1A. Brightfield images show that both cell lines successfully generated breast tumor spheroids starting from day 3 (Fig. 1B). The MDA-MB-231 tumor spheroids showed uniformed growth, became more rounded, and demonstrated significant compactness as the diameter reduced on days 12 and 15. MCF-7 tumor spheroids, in contrast, were not uniform in shape and demonstrated an increase in the diameter on days 12 and 15 (Fig. 1C). These differences in growth might be attributed to the different nature of the two cell lines, likely stemming from different single-cell interaction within the tumor spheroids and the amount of E-cadherin produced by each tumor spheroids [27]. Diameters between 2–2.5 mm^3 and 0.5–1 mm^3 were selected for further experiments for both MDA-MB-231 tumor spheroids and MCF-7 tumor spheroids, respectively.

Pharmacological doses of Vit-C disrupt the MDA-MB-231 and MCF-7 tumor spheroids morphology and induce cytotoxicity

To investigate whether plain Vit-C could induce a cytotoxic effect on two BC tumor spheroids (MDA-MB-231 and MCF-7) as previously described [28], we selected five pharmacological concentrations of high-dose Vit-C (1, 5, 10, 15, and 20 mM). After 72 h, Vit-C largely disrupted the morphology and induced cytotoxicity in both spheroids in a dose-dependent manner (Fig. 2A). Notably, compared with other doses, the 20 mM produced the severest morphological disintegration in both cancer spheroids. Although the effects were most pronounced after 72 h, the outer cellular debris formation and the residual spheroidal body generation started from 24 h after Vit-C administration (Fig. 2A).

Next, we wanted to see if the observable cytotoxicity in both tumor spheroids was due to high-dose Vit-C-induced ATP depletion. For that purpose, after 72 h of Vit-C treatment with the designated doses, we used CellTiter-Glo® 3D Cell Viability Assay, which is a homogenous compound that determines the viable cell numbers present in 3D tumor spheroids based on the quantification of the ATP (which is a characteristic of metabolically active cells) by generating luminescent readouts. Based on the results obtained, Vit-C inhibited the MDA-MB-231 and MCF-7 spheroids growth by producing significant cytotoxicity in a dose-dependent manner compared to the vehicle control (VCTL),

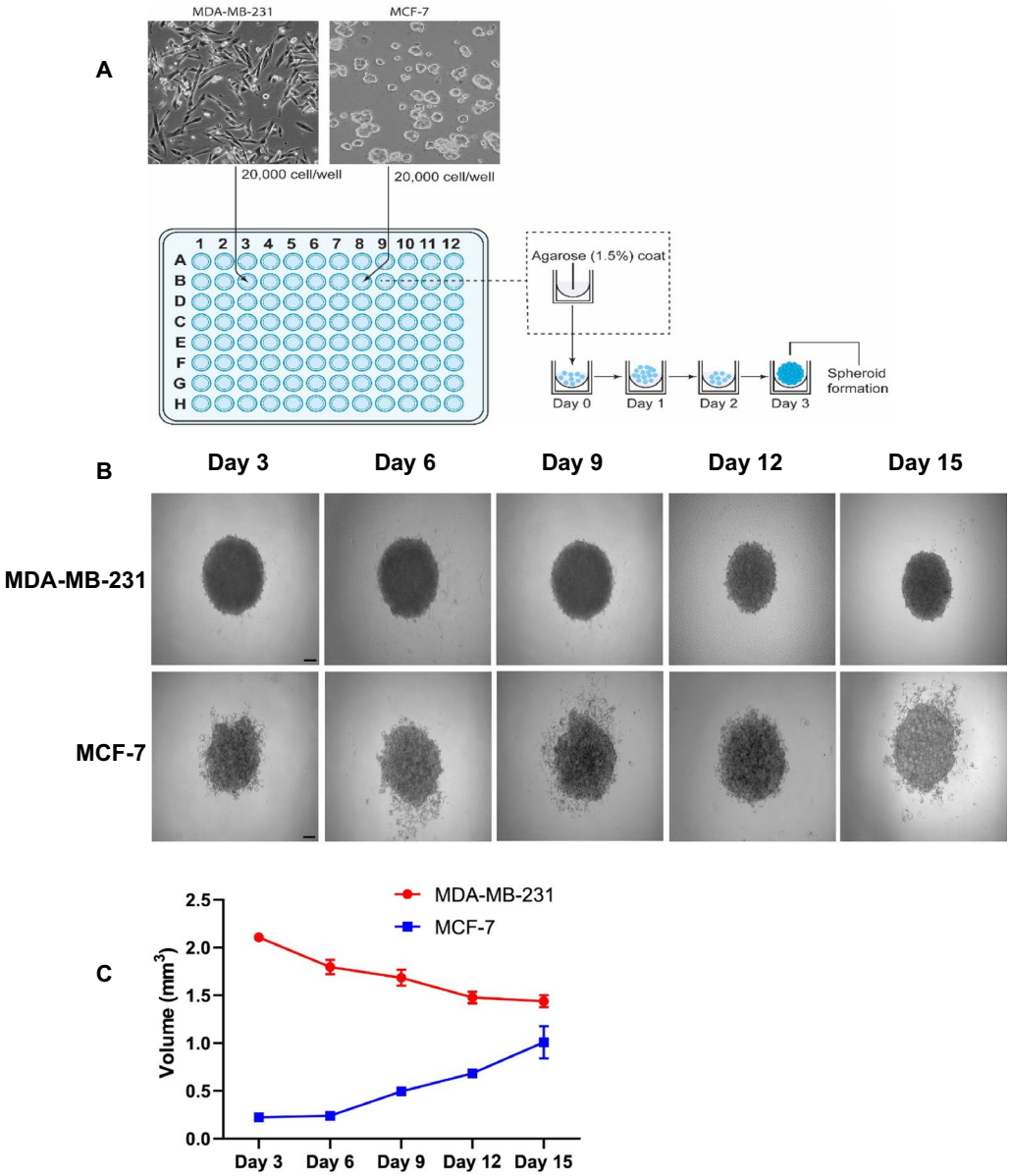

Fig. 1 Characterization of MDA-MB-231 and MCF-7 Tumor spheroids. **A** Schematic diagram showing the protocol utilized to develop MDA-MB-231 and MCF-7 tumor spheroids. **B** Representative brightfield images for the growth kinetics of the MDA-MB-231 and MCF-7 tumor spheroids. Cells at the density of 2×10^4 cells/well were seeded in a 96-well agarose-coated plate and incubated over a period of 15 days. Images were acquired starting from day 3 from seeding to day 15. Scale bars = 500 µM; all images are of the same resolution. **C** A graph showing the growth kinetics of MDA-MB-231 and MCF-7 tumor spheroids, where the diameter of MDA-MB-231 tumor spheroids decreased with time, as compared to MCF-7 tumor spheroids, for which the diameter increased with time

and the cytotoxic effect of 20 mM was superior to that of the other Vit-C doses (Fig. 2B, C). MDA-MB-231 spheroids (Fig. 2B) experienced a more severe cytotoxic effect compared to MCF-7 spheroids (Fig. 2C), indicating that Vit-C could not only target the non-aggressive BC, represented by MCF-7 spheroids, but also more effectively target the aggressive form of BC, represented by MDA-MB-231 spheroids.

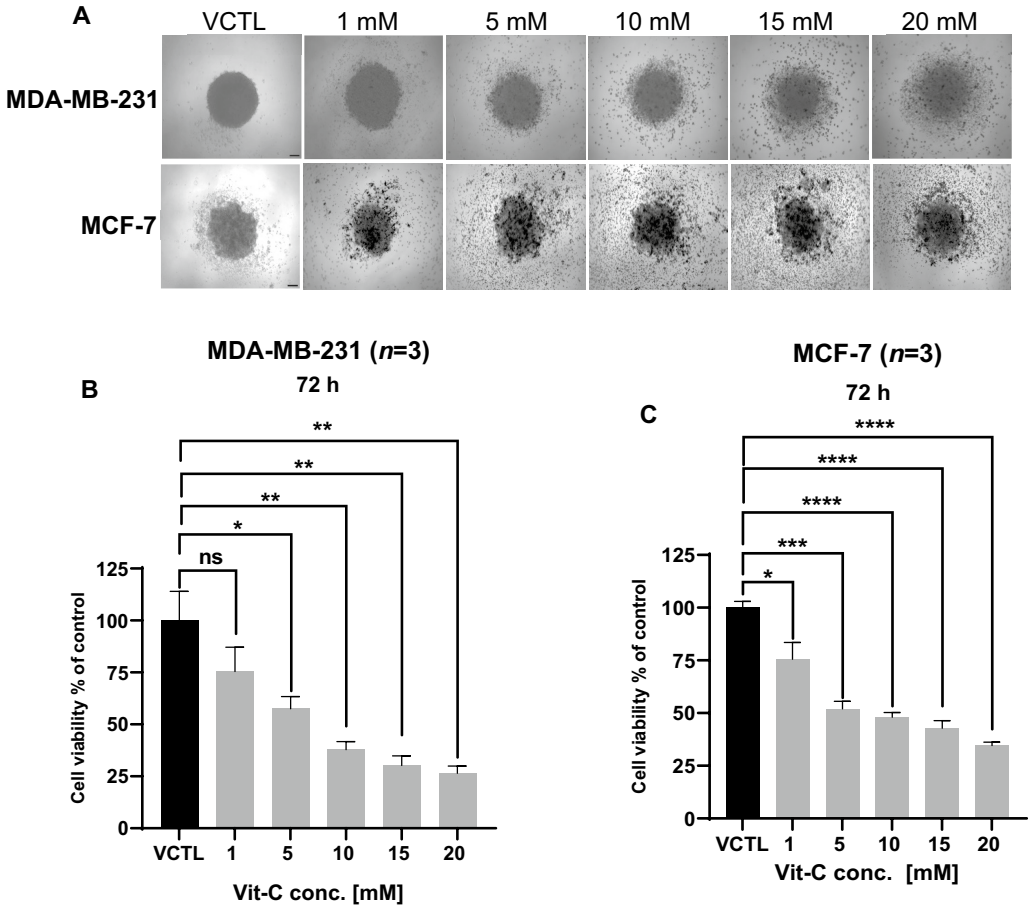

Fig. 2 Pharmacological doses of Vit-C induce cytotoxicity of MDA-MB-231 and MCF-7 spheroids. **A** After successfully generating MDA-MB-231 and MCF-7 spheroids, five pharmacological doses of Vit-C (1 mM, 5 mM, 10 mM, 15 mM, and 20 mM) were used to treat each spheroid for 72 h, while the vehicle control (VCTL) was treated with ddH_2O. Representative brightfield images were captured for each spheroid after treatment to show that Vit-C induced morphological disintegration in both tumor spheroids in a dose-dependent manner. Scale bars = 500 µM; all images are of the same resolution. **B** and **C** Cell viability analysis after treatment of MDA-MB-231 and MCF-7 spheroids with five pharmacological doses of Vit-C (1, 5, 10, 15, and 20 mM) for 72 h. In MDA-MB-231 and MCF-7 spheroids, the cytotoxic effect of Vit-C was dose-dependent (**B** and **C**). The statistical significance levels were determined as follows: $^{**}P < 0.01$, $^{***}P < 0.001$, $^{****}P < 0.0001$, and $^{*}P < 0.05$, ns, not significant. Two-tailed unpaired student's *t*-test was employed in both cases, and the error bars describe the mean ± SEM; data represent three independent experiments ($n = 3$)

(See figure on next page.)

Fig. 3 Pharmacological doses of Vit-C generate high H_2O_2 concentrations. **A** Schematic diagram showing the mechanism of vitamin C (Vit-C)-mediated hydrogen peroxide (H_2O_2) production via the Fenton reaction and the Haber–Weiss reaction. The transition of Vit-C between ascorbic intermediate radical ($Asc^{\bullet-}$) and dehydroascorbic acid (DHA) can lead to H_2O_2 production in the extracellular environment, which can rapidly diffuse inside the BC cell. Following the entrance of $Asc^{\bullet-}$ via sodium-dependent Vit-C transporter (SVCT) and DHA via glucose transporter 1 (GLUT-1), they utilize the transition labile iron pool (LIP, Fe^{2+}) in addition to the reduction of reduced glutathione (GSH) to glutathione disulfide (GSSG) by DHA in the presence of NADPH to produce massive amounts of intracellular hydrogen peroxide (H_2O_2), hydroxide ion (OH^-), hydroxyls radical ($^{\bullet}OH$), and superoxide ($O_2^{\bullet-}$). This, in turn, will activate caspases 3 and 7, leading to cancer cell death by apoptosis. **B** and **C** H_2O_2 level measurement in MDA-MB-231 and MCF-7 spheroids after the treatment with five pharmacological doses of Vit-C (1 mM, 5 mM, 10 mM, 15 mM, and 20 mM) for 72 h, respectively. The levels of H_2O_2 production were Vit-C dose-dependent in MDA-MB-231 tumor spheroids and MCF-7 tumor spheroids, respectively (**B** and **C**). **D** and **E** Cell viability analysis of MDA-MB-231 and MCF-7 tumor spheroids treated with CAT (300 U/mL) for 2 h, then supplemented with five pharmacological doses of Vit-C (1, 5, 10, 15, and 20 mM) for 72 h. The statistical levels of significance were determined as follows: $^{**}P < 0.01$, $^{***}P < 0.001$, $^{****}P < 0.0001$, and $^{*}P < 0.05$. Two-tailed unpaired student's *t*-test was employed in both cases, and the error bars represent the mean ± SEM; the data are representation of three independent experiments ($n = 3$)

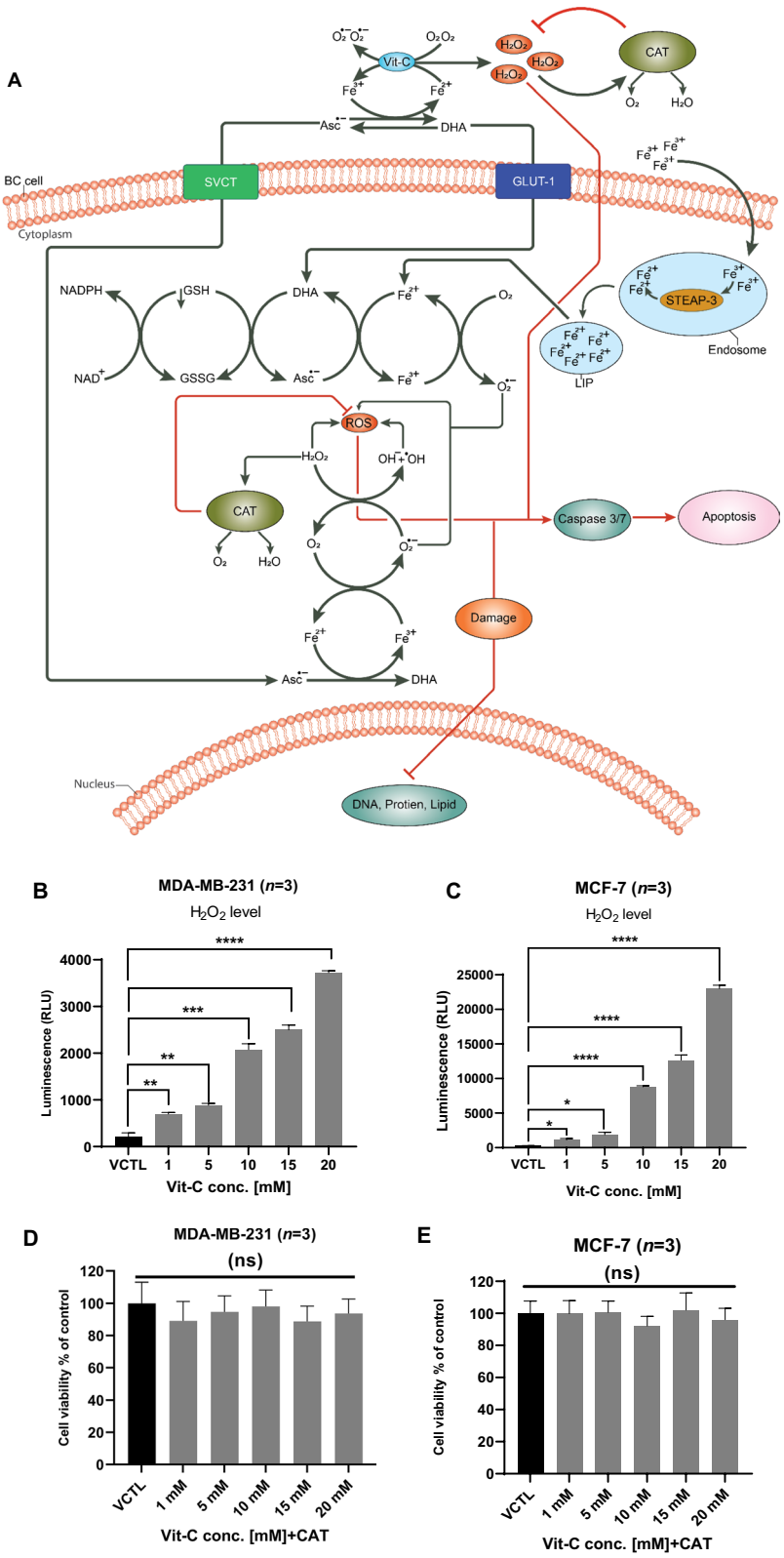

Fig. 3 (See legend on previous page.)

Pharmacological doses of Vit-C induce cytotoxicity in MDA-MB-231 and MCF-7 tumor spheroids by generating ROS

We wanted to investigate if the cytotoxic effect mediated by the pharmacologically high-doses of Vit-C on both BC tumor spheroids was due to generation of high H_2O_2 concentrations (Fig. 3A). After 72 h of Vit-C treatment with the designated doses, we used the ROS-GLO™ H_2O_2 ASSAY to measure the total H_2O_2 concentration. The data show that all Vit-C concentrations, especially 10, 15, and 20 mM, produced significant concentrations of H_2O_2 compared to the control. Moreover, the concentrations increased in a dose-dependent manner in both BC tumor spheroids (Fig. 3). In comparison to MDA-MB-231 tumor spheroids shown in Fig. 3B, the H_2O_2 generation induced by Vit-C was more significant in MCF-7 tumor spheroids, as depicted in Fig. 3C. This suggests that MCF-7 breast spheroids exhibit a greater susceptibility to Vit-C-induced cell death, whereas the aggressive MDA-MB-231 spheroids displayed a lower sensitivity. We next aimed to confirm whether the concentrations of H_2O_2 generated are responsible for Vit-C-mediated BC tumor spheroids cell death. To this end, we added catalase (CAT, EC Number: 1.11.1.6), a key antioxidant enzyme that protects the cells from H_2O_2-mediated cellular damage by converting the H_2O_2 to water and oxygen [21]. Next, the cell viability was assessed. Interestingly, prior treatment with CAT (600 U/mL) for 2 h effectively prevented the production of H_2O_2 by Vit-C and preserved the viability of both BC spheroids (Fig. 3D and E).

Furthermore, the mechanism of Vit-C-mediated intracellular H_2O_2 production necessitates the depletion of GSH (Fig. 3A) [29, 30]. Given this, we conducted measurements of GSH and GSSG levels to analyze the GSH/GSSG ratio after 72 h of treatment with designated doses of Vit-C on both tumor spheroids. Our aim was to examine whether Vit-C has the potential to disturb GSH homeostasis as previously reported [29, 30]. Remarkably, Vit-C treatment led to a noticeable decrease in the GSH to GSSG ratio in a dose-dependent manner in both BC spheroids compared to VCTL (Fig. 4). However, MCF-7 tumor spheroids (Fig. 4A) exhibited a more pronounced decrease in the GSH-to-GSSG ratio compared to MDA-MB-231 tumor spheroids (Fig. 4B). Still, the results indicate that Vit-C can cause an imbalance in GSH levels in both spheroid types leading to sever oxidative stress state.

H_2O_2 generated by pharmacological Vit-C induce apoptotic cell death in MDA-MB-231 and MCF-7 spheroids

To validate whether Vit-C-mediated H_2O_2 can induce apoptosis, first we used flow cytometry to detect Annexin V-FITC and propidium iodide (PI) and assess the level of apoptotic cell death in Vit-C-treated tumor spheroids as well as in VCTL spheroids. As depicted in Fig. 5A

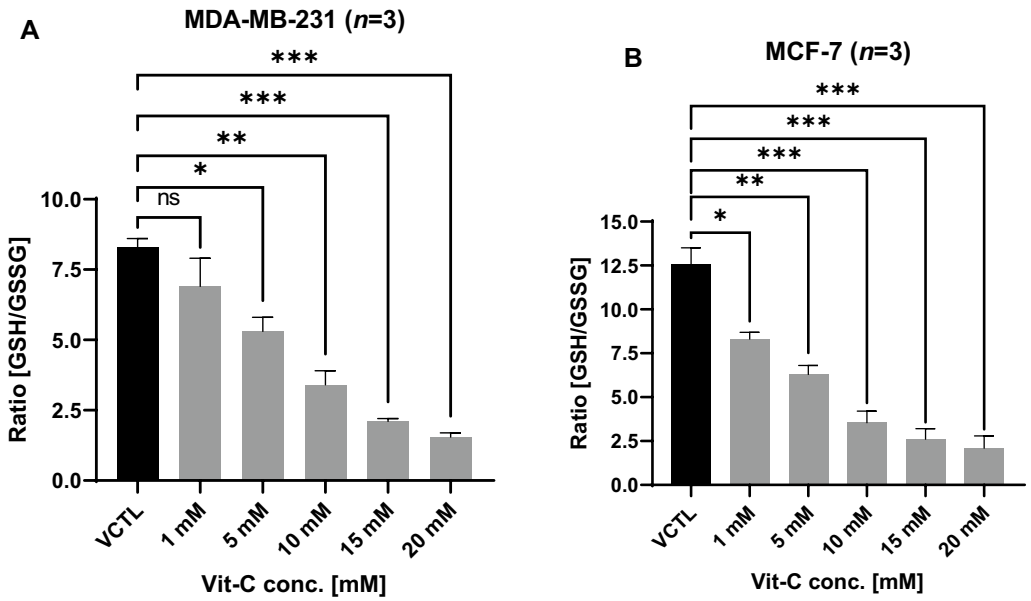

Fig. 4 Pharmacological doses of Vit-C induce GSH/GSSG imbalance. **A** and **B** show the GSH/GSSG ratio analysis by using the GSH/GSSG-Glo™ Assay in MDA-MB-231 and MCF-7 spheroids after treatment with five pharmacological doses of Vit-C (1, 5, 10, 15, and 20 mM) for 72 h, respectively. The levels of the statistical significance were determined as follows: $^{**}P < 0.01$, $^{***}P < 0.001$, $^{****}P < 0.0001$, and $^{*}P < 0.05$, ns, not significant. One way ANOVA was employed in both cases, and the error bars represent the mean ± SEM. The data are representative of three independent experiments ($n = 3$)

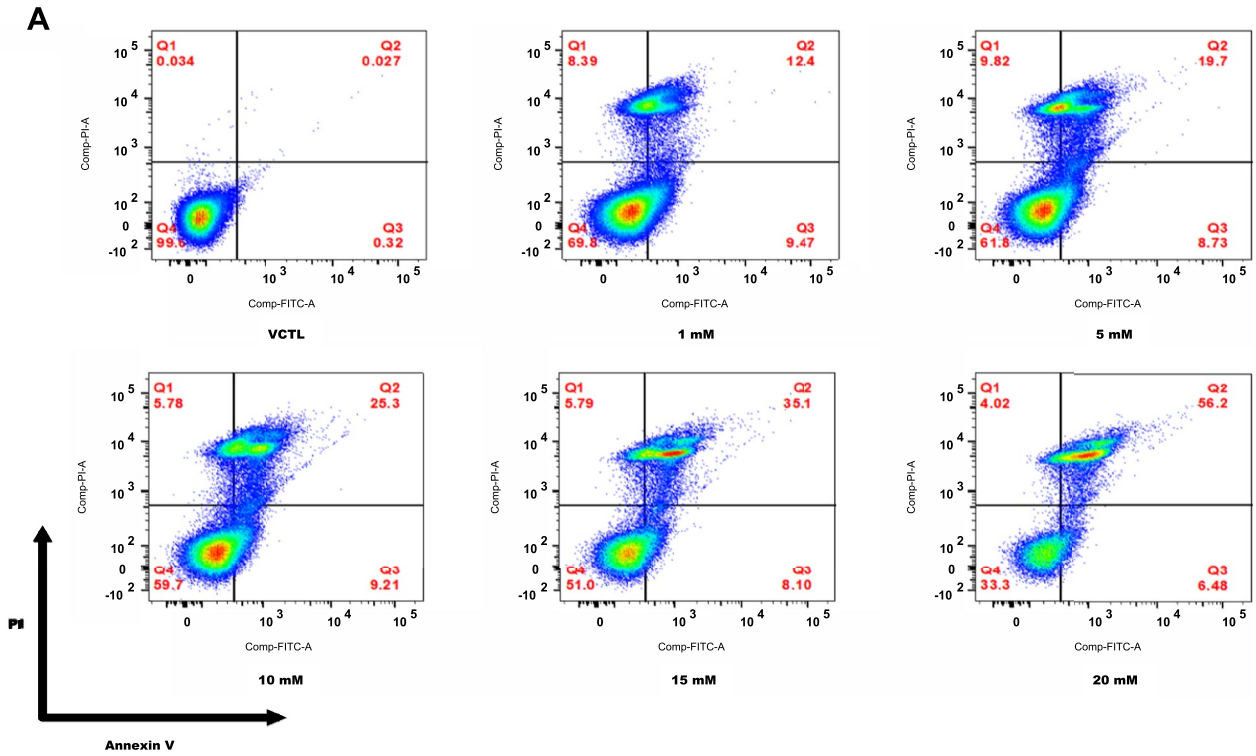

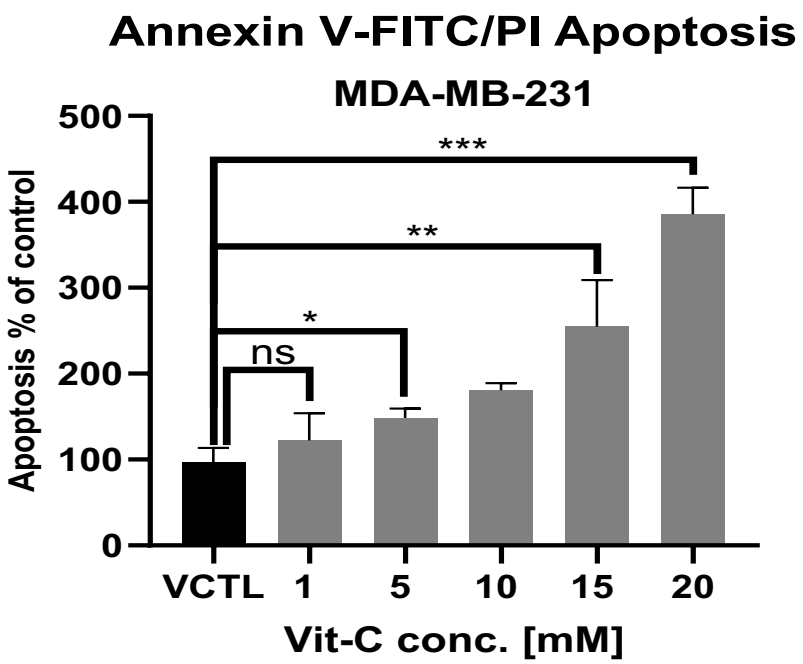

Fig. 5 Pharmacological doses of Vit-C induce apoptosis in MDA-MB-231 and MCF-7 spheroids. **A** and **B** Flow cytometry analysis by using Annexin V-FITC/PI staining to measure apoptosis in MDA-MB-231 and MCF-7 spheroids after treatment with five pharmacological doses of Vit-C (1, 5, 10, 15, and 20 mM) for 72 h, respectively. **C** and **B** Caspase-3/7 activity measurement by Caspase-Glo® 3/7 3D Assay in MDA-MB-231 and MCF-7 spheroids subjected to treatment with five pharmacological concentrations of Vit-C (1, 5, 10, 15, and 20 mM) for 72 h, respectively. The levels of the statistical significance were determined as follows: $^{**}P < 0.01$, $^{***}P < 0.001$, $^{****}P < 0.0001$, and $^{*}P < 0.05$, ns, not significant. Two-tailed unpaired student's *t*-test was employed in both cases, and the error bars represent the mean ± SEM. The data are representative of three independent experiments ($n = 3$)

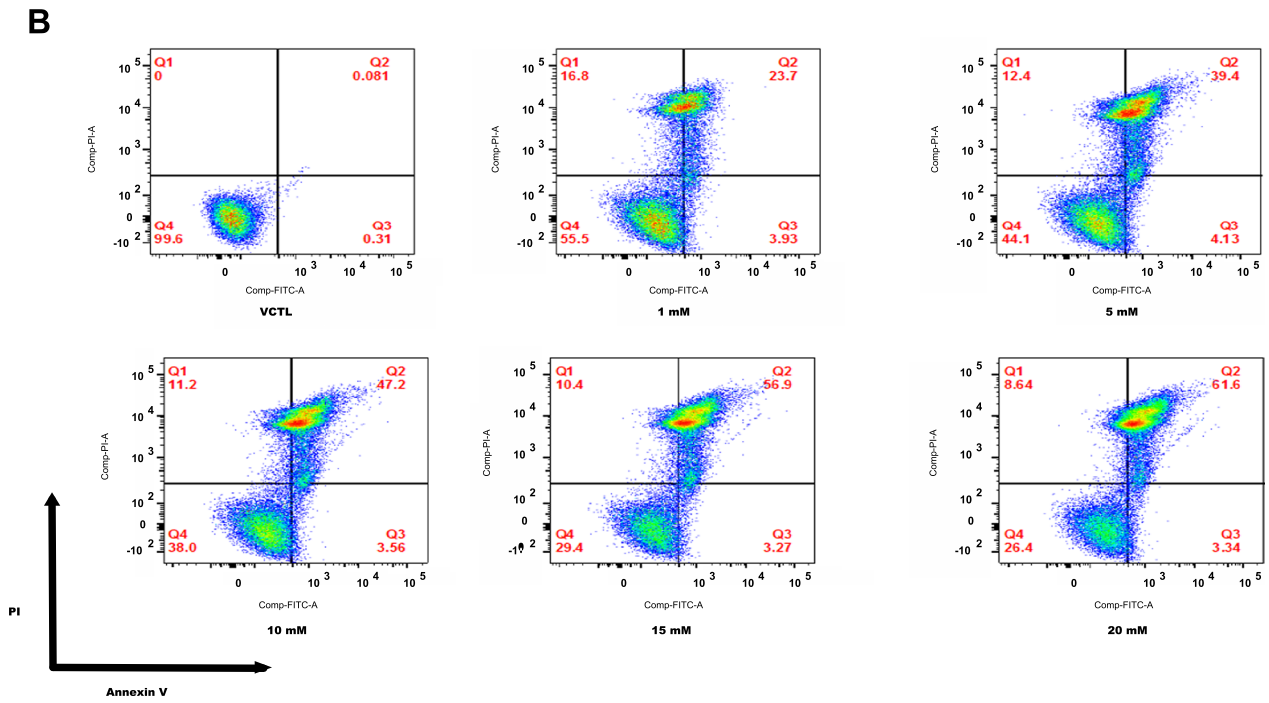

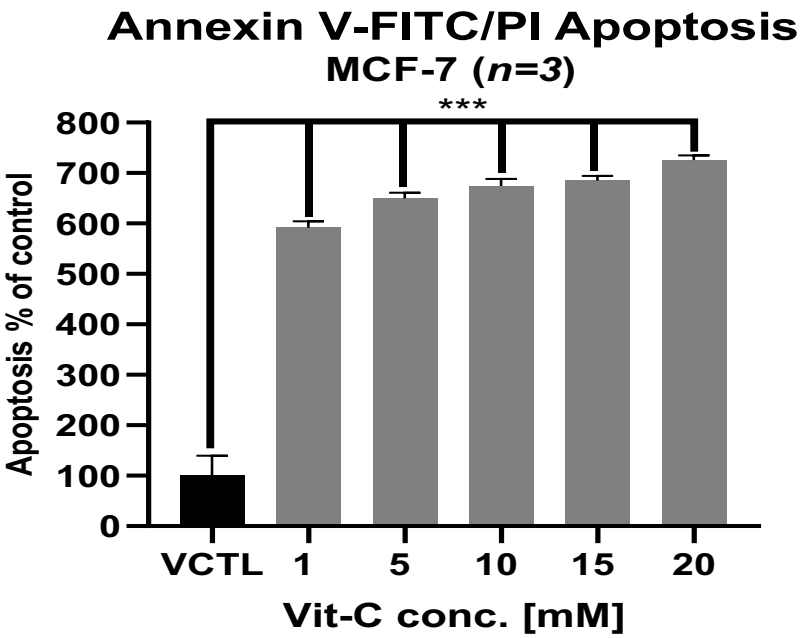

Fig. 5 continued

and Fig. 5B, the cells were categorized into four populations: Annexin V-/P- (live), Annexin V + /P− (early apoptosis), Annexin V + /P + (late apoptosis), and Annexin V-/P + (necrosis). We combined the early and the late apoptotic population into total apoptotic population and excluded the necrotic cells from the analysis because our focus was only on assessing Vit-C-mediated apoptosis. As previously described, we administered different concentrations of Vit-C to MDA-MB-231 and MCF-7 tumor spheroids. As shown in Fig. 5A and B, we observed a dose-dependent increase in the percentage of apoptotic cells in both tumor spheroids. For MDA-MB-231 tumor

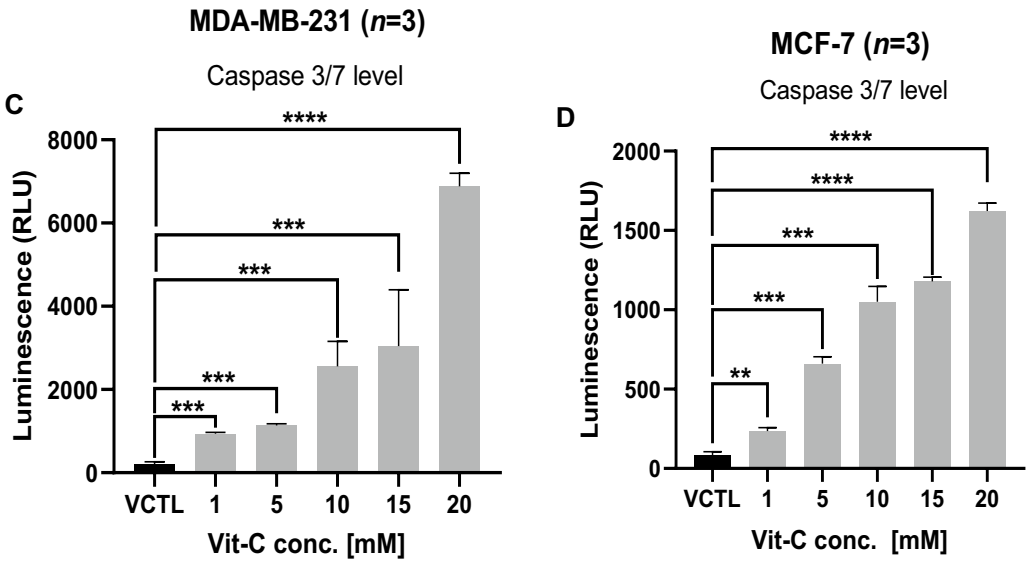

Fig. 5 continued

spheroids, with higher drug concentrations reaching a maximum at 20 mM, there was a significant increase in apoptosis (Fig. 5A). Similarly, MCF-7 tumor spheroids experienced a dose-dependent increase in apoptosis, with 20 mM inducing the highest percentage of cellular apoptotic death (Fig. 5B). The statistical analysis confirmed that the increases in apoptosis at each concentration were significant compared to the control ($P < 0.05$). The results indicate that Vit-C induces apoptotic cell death in a dose-dependent manner.

To confirm the apoptosis results obtained from the Annexin V-FITC and PI flow cytometry analyses, we measured the activity of caspase-3/7 in both tumor spheroids by using the Caspase-Glo® 3/7 3D assay (Fig. 5C and D). MDA-MB-231 and MCF-7 tumor spheroids were subjected to treatment with Vit-C as described previously, and then the activity of caspase-3/7 was quantified. As expected, Vit-C augmented the activity of caspase-3/7 in a dose-dependent manner in both BC tumor spheroids (Fig. 5C and D). In MDA-MB-231 tumor spheroids, the activity of caspase-3/7 was significantly elevated at 5 mM Vit-C and higher concentrations, with the highest activity observed at 20 mM (Fig. 5C). MCF-7 spheroids also demonstrated elevated levels of caspase-3/7 in a dose-dependent manner, with the significant increase starting at 5 mM and peaking at 20 mM (Fig. 5D). The statistical analysis confirmed that the increases in apoptosis at each concentration were significant compared to the control ($P < 0.05$). Moreover, the results supported the data obtained from the previous experiments involving Annexin V-FITC and PI, indicating that the production of H_2O_2 mediated by Vit-C can cause apoptotic cell death in a dose-dependent manner in both BC spheroids. In addition, the strong correlation between the Annexin V-FITC/PI staining results obtained by flow cytometry and the caspase-3/7 activity data enhance the credibility of our findings. As anticipated, the results of our study demonstrate that Vit-C-induced H_2O_2 generation is a potent trigger of apoptosis, ultimately resulting in BC spheroids death.

Discussion

Pharmacokinetic studies suggested that the plasma concentration of pharmacological Vit-C could range from 0.3 to 20 mM when supplied intravenously without producing noticeable off-target cytotoxic effects [31–33]. These concentrations of Vit-C were found to produce cellular cytotoxicity via the induction of tremendous amounts of ROS, which selectively kill cancer cells while not affecting normal cells [31, 32, 34, 35]. This indicates that tumor cells are deficient in ROS detoxifying mechanisms, which could mitigate the impact of ROS-induced cancer cell death.

A recent study demonstrated that Vit-C (5–20 mM) caused cytotoxicity through elevated ROS production in three modules of osteosarcoma tumor spheroids, while the direct addition of DHA and $Asc^{\bullet-}$ exhibited minimal cytotoxic effects in comparison to Vit-C [28]. This indicates that the processing of Vit-C under standard physiological conditions is essential for achieving its optimal cytotoxic effect mediated by ROS. In a 2D BC cell culture, a concentration between 5 and 20 mM was found to induce a significant cytotoxic effect on the cancerous MDA-MB-231, SK-BR3, and MCF-7 cell lines, while the

non-cancerous cell line MCF-10A remained unaffected [25]. As a result, for our study we selected five different Vit-C concentrations to match this range: 1, 5, 10, 15, and 20 mM. Pharmacological Vit-C at these concentrations triggered severe morphological disintegration and cellular deformities in both tumor spheroids, as well as significant cytotoxicity. The results presented here are consistent with earlier findings in 2D BC cell culture, which demonstrated that high concentrations of Vit-C led to significant cellular cytotoxicity and morphological disintegration [22, 25, 36, 37]. The findings align with a recent study indicating that higher concentrations of Vit-C especially 20 mM resulted in significant cellular disintegration in osteosarcoma tumor spheroids [28]. In a previous 2D, BC cell culture investigation, elevated concentrations of Vit-C (10 mM or 20 mM) induced cytotoxic effects in MCF-7 cells, whereas MDA-MB-231 cells remained unaffected [38]. In contrast, we have observed that both of these BC cell lines to be susceptible to Vit-C in these concentration regimens when adopting the form of tumor spheroids. This suggests that pharmacological Vit-C is effective not only against MCF-7 but also targets MDA-MB-231 spheroids associated with triple-negative breast cancer (TNBC) effectively.Vit-C can induce cytotoxicity in cancer cells through diverse mechanisms, some of which, studied herein, can be attributed to ATP depletion and H_2O_2-mediated apoptosis. Our results align with other previous studies that have found that pharmacological Vit-C can cause a significant reduction in ATP levels via over-activation of PARP-mediated NAD^+ depletion, thus inhibiting GADPH and ultimately resulting in cell death by disrupting tumor cell metabolism, notably glycolysis in a number of cancer models, including BC [22, 35, 39–44]. This suggests that Vit-C can induce selective cytotoxicity as a result of metabolic stress in BC cells, that rely heavily on ATP as their primary source of energy.

Furthermore, in addition to depleting ATP, pharmacological Vit-C generates high levels of ROS, leading to apoptotic cancer cell death [28, 29, 31]. In this regard, H_2O_2 is a remarkably stable molecule in the ROS group and regarded as one of the main players in Vit-C-induced cytotoxicity. It efficiently diffuses through the cellular membrane upon extracellular generation, resulting in the induction of severe oxidative stress [45]. Vit-C-mediated killing of cancer cells depends on the ability to produce sufficient concentrations of H_2O_2, inside the cells as well as in the extracellular environment. This H_2O_2 production proceeds Vit-C autoxidation ($Asc^{\bullet-}$/DHA) in the media by free radicals [28, 29, 31]. Vit-C uses the transition metal labile iron pool (ferrous iron; Fe^{2+}) produced from the reduction of ferric iron (Fe^{3+}) by the endosomal-six transmembrane-epithelial antigen of prostate-3 (STEAP-3) in the endosome to generate H_2O_2 through the Fenton reaction and the Haber–Weiss reaction [21, 28, 29, 31]. Consistent with prior studies, we observed a significant production of H_2O_2 in both spheroids when exposed to pharmacological doses of Vit-C [22, 29, 31, 35, 36, 39, 41, 46].

Catalase (CAT) is a known antioxidant enzyme that mediates H_2O_2 detoxification by catalyzing its conversion into water and oxygen [21, 28, 45, 47]. To confirm if the action of pharmacological Vit-C-mediated H_2O_2 generation could lead to the death of the two BC tumor spheroids, we dosed the cells with CAT prior to the administration of Vit-C. This prior addition of extracellular CAT completely inhibited the death of the two spheroids, indicating their sensitivity to pharmacological Vit-C-mediated H_2O_2 generation and thus confirming the contribution of H_2O_2 in the observed cytotoxicity mediated by Vit-C. The results we obtained are consistent with previous findings that reached the same conclusions in 2D cell culture and tumor spheroids [22, 28, 29, 31, 45, 47]. These findings indicate that both BC spheroids have an extremely low expression of CAT, which may be responsible for their high sensitivity to pharmacological Vit-C-mediated H_2O_2 cell death. However, further investigations are needed to determine if the low expression of other antioxidant enzymes is also involved.

Given that pharmacological Vit-C-mediated H_2O_2 generation can lead to redox imbalance, we also analyzed the GSH/GSSG ratio in our spheroids. The results of this analysis confirmed a significant decrease in the ratio of GSH to GSSG in both BC tumor spheroids, which aligns with previous findings [22, 28, 46, 47]. Moreover, data from previous studies reported that Vit-C can lead to cancer cell death via oxidative stress-induced activation of caspases, in addition to other pathways such as ferroptosis, TRAIL-induced apoptosis, metabolic disruption, and necrosis [22, 29, 31, 35, 44, 48–52]. In the oxidative stress-mediating cancer cell killing pathway, Vit-C-mediated H_2O_2 can inhibit anti-apoptotic protein, B cell lymphoma 2 (Bcl-2), can activate Bax (a well-known pro-apoptotic mediator), can induce mitochondrial hyperpolarization, can stimulate the poly (ADP-ribose) polymerase (PARP, a known apoptotic indicator) cleavage, and the cleavage of caspases, mainly caspases 3 and 7, ultimately leading to cancer cell death by apoptosis [22, 41–43, 53, 54]. In our study, Vit-C treatment significantly induced apoptotic death of both tumor spheroids via high concentrations of H_2O_2-mediated caspase 3/7 activation. The results are consistent with previous research, supporting the notion that Vit-C possesses potent apoptotic properties in targeting cancer cell [22, 28, 46, 47, 53]. It should be noted that, the exact mechanism of how Vit-C activates caspase 3/7 through H_2O_2 is not

completely understood, nor is it clear whether the signal needed to trigger apoptosis is intrinsic (i.e., mitochondrial) or extrinsic. However, studies indicate that treatment with Vit-C leads to the cleavage of caspase 8, which suggests the presence of an extrinsic apoptotic signal [3]. This indicates the necessity for further investigation to identify all the potential apoptotic pathways that may be triggered by Vit-C.

This work demonstrates the improved effectiveness of high-dose Vit-C by the use of BC tumor spheroids, consistent with current developments in 3D culture technology. This in turn, provides a comprehensive realistic assessment of response to drugs and highlight a potential for clinical translation.

Conclusions

Our study demonstrates that pharmacological Vit-C effectively induces cytotoxicity in both non-aggressive (MCF-7) and aggressive (MDA-MB-213) forms of BC tumor spheroids at various concentrations. The main cause of cytotoxicity induced by Vit-C is the production of H_2O_2. Significant levels of H_2O_2 can cause apoptosis and impose damage to DNA, lipids, and proteins. The presence of high concentrations of H_2O_2, induced by Vit-C in a dose-dependent manner, resulted in the activation of caspase-3 and caspase-7, which directly promoted the apoptosis. The key role of H_2O_2 in mediating apoptosis was confirmed by reversing the cytotoxic action of Vit-C when the H_2O_2 inhibitor, CAT was incorporated into the external cellular environment. The impact of Vit-C on the destruction of the tumor cells varied slightly between the two spheroids, yet in contrast to previous literature using 2D models, it demonstrated the ability of Vit-C to target both forms of BC effectively. The observed subtle mechanistic variations could be attributed to the characteristics of the BC cell lines employed, underscoring the importance of evaluating different molecular subtypes of BC.

Given the robust results obtained on our two tumor spheroid models and the significant cytotoxic impact of Vit-C, we urge fellow researchers to explore the effects of Vit-C on spheroids of different cancers, as well as in more advanced models, such as tumor organoids alone or with different combinatorial cancer treatments. This will allow us to go beyond the current limitations in the therapeutic efficiency of Vit-C as an anticancer modality. Currently, Vit-C is only used as a supplementary therapy, while its use as a standalone treatment has not advanced pass the preclinical stage. However, with deepening insight with regard to the anticancer effect of Vit-C on the molecular level, these impasses may be overcome to take it from bench to bedside.

Abbreviations

Vit-C	Vitamin C
BC	Breast cancer
GSH	Reduced glutathione
GSSG	Glutathione disulfide
TME	Tumor microenvironment
3D	3-Dimensional
2D	2-Dimensional
ROS	Reactive oxygen species
OH^-	Hydroxide ion.
NF-κB	Nuclear factor kappa beta of activated b cells
H_2O_2	Hydrogen peroxide
$^{\cdot}OH$	Hydroxyl radical
$O_2^{\cdot -}$	Superoxide
LIP	Labile iron pool
$Asc^{\cdot -}$	Ascorbic intermediate radical
DHA	Dehydroascorbic acid
SVCT	Sodium-dependent Vit-C transporter
GLUT-1	Glucose transporter 1
CAT	Catalase
Fe^{2+}	Ferrous iron
Fe^{3+}	Ferric iron
STEAP-3	Endosomal-six transmembrane-epithelial antigen of prostate-3
Bcl-2	B cell lymphoma 2
PARP	Poly (ADP-ribose) polymerase

Acknowledgements

A.M. would like to acknowledge the Universiti Sains Malaysia (USM) GRA-Assistant Scheme for providing financial support, and the Sudanese Researcher Community for technical support. We would also like to thank Dr. Mustafa Talib for his positive comments regarding our manuscript.

Author contributions

Conceptualization, A.M., R.H., R.M.; Writing—Original draft preparation, A.M., M.H., A.H.M.; Artwork, A.M.; Writing—Review and Editing, R.M., K.H., M.A.I.A., N.F.M., V.U, M.P. and R.H.; Supervision and Funding acquisition, R.H., R.M. All authors have read and agreed to the published version of the manuscript.

Funding

This work was funded by the Ministry of Higher Education Malaysia for Fundamental Research Grant Scheme (FRGS) with Project Code: FRGS/1/2019/SKK08/USM/01/2.

Availability of data and materials

Not applicable.

Declarations

Ethics approval and consent to participate

Not applicable.

Consent for publication

Not applicable.

Competing interests

The authors declare no competing of interests.

Author details

[1]Department of Haematology, School of Medical Sciences, Universiti Sains Malaysia, Kubang Kerian, 16150 Kelantan, Malaysia. [2]Department of Biology, Faculty of Education, Omdurman Islamic University, P.O. Box 382, Omdurman, Sudan. [3]Department of Pharmaceutics, Xiangya School of Pharmaceutical Sciences, Central South University, Changsha 410013, Hunan, China. [4]Department of Zoology, Faculty of Sciences and Information Technology, University of Nyala, Nyala 63311, Sudan. [5]Department of Zoology, Faculty of Science and Technology, Omdurman Islamic University, P. O. Box 382, Omdurman, Sudan. [6]Institute for Research in Molecular Medicine (INFORMM), Universiti Sains Malaysia, Health Campus, Kubang Kerian, 16150 Kelantan, Malaysia. [7]UPMC Hillman Cancer Center, Division of Malignant Hematology and Medical Oncology, Department of Medicine, University of Pittsburgh School

of Medicine, Pittsburgh, PA 15224, USA. [8]Advanced Materials and Nanobiotechnology Laboratory, TardigradeNano LLC, Irvine, CA 92604, USA. [9]Division of Natural Sciences, Fullerton College, 321 East Chapman Avenue, Fullerton, CA 92832, USA. [10]The Accelerator for Translation in Clinical Trials (ATRACT) Centre, School of Health and Biomedical Sciences, RMIT University, Melbourne, VIC 3083, Australia. [11]Department of Immunology, School of Medical Sciences, Universiti Sains Malaysia, Kubang Kerian, 16150 Kelantan, Malaysia. [12]Institute for Research in Molecular Medicine, Universiti Science Malaysia, Health Campus, 16150 Kota Bharu, Kelantan, Malaysia. [13]Department of Medical Microbiology and Immunology, College of Medicine and Health Sciences, United Arab Emirates University, Al Ain, UAE.

Received: 23 November 2024 Accepted: 18 December 2024
Published online: 08 January 2025

References

1. Sung H, Ferlay J, Siegel RL, et al. Global cancer statistics 2020: GLOBOCAN estimates of incidence and mortality worldwide for 36 cancers in 185 countries. CA A Cancer J Clin. 2021;71(3):209–49. https://doi.org/10.3322/caac.21660.
2. Siegel RL, Giaquinto AN, Jemal A. Cancer statistics, 2024. CA A Cancer J Clin. 2024;74(1):12–49. https://doi.org/10.3322/caac.21820.
3. Darwiche W, Gomila C, Ouled-Haddou H, et al. 1, Ascorbic acid (vitamin C) synergistically enhances the therapeutic effect of targeted therapy in chronic lymphocytic leukemia. J Exp Clin Cancer Res. 2020;39(1):228. https://doi.org/10.1186/s13046-020-01738-0.
4. Debien V, De Caluwé A, Wang X, et al. Immunotherapy in breast cancer: an overview of current strategies and perspectives. NPJ Breast Cancer. 2023;9(1):7. https://doi.org/10.1038/s41523-023-00508-3.
5. Place AE, Jin Huh S, Polyak K. The microenvironment in breast cancer progression: biology and implications for treatment. Breast Cancer Res. 2011;13(6):227. https://doi.org/10.1186/bcr2912.
6. Tiwari A, Trivedi R, Lin S-Y. Tumor microenvironment: barrier or opportunity towards effective cancer therapy. J Biomed Sci. 2022;29(1):83. https://doi.org/10.1186/s12929-022-00866-3.
7. Kapałczyńska M, Kolenda T, Przybyła W, et al. 1, 2D and 3D cell cultures—a comparison of different types of cancer cell cultures. Arch Med Sci. 2018;14(4):910–9. https://doi.org/10.5114/aoms.2016.63743.
8. Han K, Pierce SE, Li A, et al. 1, CRISPR screens in cancer spheroids identify 3D growth-specific vulnerabilities. Nature. 2020;580(7801):136–41. https://doi.org/10.1038/s41586-020-2099-x.
9. Giusti I, Poppa G, D'Ascenzo S, et al. Cancer three-dimensional spheroids mimic in vivo tumor features, displaying "inner" extracellular vesicles and vasculogenic mimicry. Int J Mol Sci. 2022. https://doi.org/10.3390/ijms231911782.
10. Kuen J, Darowski D, Kluge T, et al. Pancreatic cancer cell/fibroblast co-culture induces M2 like macrophages that influence therapeutic response in a 3D model. PLoS ONE. 2017;12(7): e0182039. https://doi.org/10.1371/journal.pone.0182039.
11. Kasper SH, Morell-Perez C, Wyche TP, et al. Colorectal cancer-associated anaerobic bacteria proliferate in tumor spheroids and alter the microenvironment. Sci Rep. 2020;10(1):5321. https://doi.org/10.1038/s41598-020-62139-z.
12. Singh K, Gautam PK. Macrophage infiltration in 3D cancer spheroids to recapitulate the TME and unveil interactions within cancer cells and macrophages to modulate chemotherapeutic drug efficacy. BMC Cancer. 2023;23(1):1201. https://doi.org/10.1186/s12885-023-11674-9.
13. Dhandapani H, Siddiqui A, Karadkar S, et al. In vitro 3D spheroid model preserves tumor microenvironment of hot and cold breast cancer subtypes. Adv Healthc Mater. 2023;12(21): e2300164. https://doi.org/10.1002/adhm.202300164.
14. Saraiva DP, Matias AT, Braga S, et al. 1, Establishment of a 3D co-culture with MDA-MB-231 breast cancer cell line and patient-derived immune cells for application in the development of immunotherapies. Front Oncol. 2020;10:1543. https://doi.org/10.3389/fonc.2020.01543.
15. Huang Z, Yu P, Tang J. Characterization of triple-negative breast cancer MDA-MB-231 cell spheroid model. Onco Targets Ther. 2020;13:5395–405. https://doi.org/10.2147/ott.S249756.
16. Yu J, Lu R, Nedrow JR, et al. 1, Response of breast cancer carcinoma spheroids to combination therapy with radiation and DNA-PK inhibitor: growth arrest without a change in α/β ratio. Int J Radiat Biol. 2020;96(12):1534–40. https://doi.org/10.1080/09553002.2020.1838659.
17. Leschiera E, Al-Hity G, Flint MS, et al. 1, An individual-based model to explore the impact of psychological stress on immune infiltration into tumour spheroids. Phys Biol. 2024. https://doi.org/10.1088/1478-3975/ad221a.
18. Rodriguez-Perdigon M, Haeni L, Rothen-Rutishauser B, et al. 1, Dual CSF1R inhibition and CD40 activation demonstrates anti-tumor activity in a 3D macrophage- HER2(+) breast cancer spheroid model. Front Bioeng Biotechnol. 2023;11:1159819. https://doi.org/10.3389/fbioe.2023.1159819.
19. Mougel L, Tarpin M, Albert P, et al. 1, Three-dimensional culture and multidrug resistance: effects on immune reactivity of MCF-7 cells by monocytes. Anticancer Res. 2004;24(2b):935–41.
20. Gopal S, Kwon SJ, Ku B, et al. 3D tumor spheroid microarray for high-throughput, high-content natural killer cell-mediated cytotoxicity. Commun Biol. 2021;4(1):893. https://doi.org/10.1038/s42003-021-02417-2.
21. Mussa A, Mohd Idris RA, Ahmed N, et al. High-dose Vitamin C for cancer therapy. Pharmaceuticals (Basel). 2022. https://doi.org/10.3390/ph15060711.
22. Ghanem A, Melzer AM, Zaal E, et al. Ascorbate kills breast cancer cells by rewiring metabolism via redox imbalance and energy crisis. Free Radical Biol Med. 2021;163:196–209. https://doi.org/10.1016/j.freeradbiomed.2020.12.012.
23. Mussa A, Afolabi HA, Syed NH, et al. The NF-κB transcriptional network is a high-dose Vitamin C-targetable vulnerability in breast cancer. Biomedicines. 2023. https://doi.org/10.3390/biomedicines11041060.
24. Chen W, Wong C, Vosburgh E, et al. High-throughput image analysis of tumor spheroids: a user-friendly software application to measure the size of spheroids automatically and accurately. J Vis Exp. 2014. https://doi.org/10.3791/51639.
25. Lee SJ, Jeong JH, Lee IH, et al. Effect of high-dose Vitamin C combined with anti-cancer treatment on breast cancer cells. Anticancer Res. 2019;39(2):751–8. https://doi.org/10.21873/anticanres.13172.
26. Mota AL, Evangelista AF, Macedo T, et al. Molecular characterization of breast cancer cell lines by clinical immunohistochemical markers. Oncol Lett. 2017;13(6):4708–12. https://doi.org/10.3892/ol.2017.6093.
27. Lin R-Z, Chang H-Y. Recent advances in three-dimensional multicellular spheroid culture for biomedical research. Biotechnol J. 2008;3(9–10):1172–84. https://doi.org/10.1002/biot.200700228.
28. Vaishampayan P, Lee Y. Redox-active vitamin C suppresses human osteosarcoma growth by triggering intracellular ROS-iron–calcium signaling crosstalk and mitochondrial dysfunction. Redox Biol. 2024;75:103288. https://doi.org/10.1016/j.redox.2024.103288.
29. Schoenfeld JD, Sibenaller ZA, Mapuskar KA, et al. O2·− and H2O2-mediated disruption of Fe metabolism causes the differential susceptibility of NSCLC and GBM cancer cells to pharmacological ascorbate. Cancer Cell. 2017;31(4):487-500.e8. https://doi.org/10.1016/j.ccell.2017.02.018.
30. Olney KE, Du J, vant Erve TJ, et al. Inhibitors of hydroperoxide metabolism enhance ascorbate-induced cytotoxicity. Free Radic Res. 2013;47(3):154–63. https://doi.org/10.3109/10715762.2012.755263.
31. Chen Q, Espey MG, Krishna MC, et al. 1, Pharmacologic ascorbic acid concentrations selectively kill cancer cells: action as a pro-drug to deliver hydrogen peroxide to tissues. Proc Natl Acad Sci USA. 2005;102(38):13604–9. https://doi.org/10.1073/pnas.0506390102.
32. Doskey CM, Buranasudja V, Wagner BA, et al. Tumor cells have decreased ability to metabolize H2O2: implications for pharmacological ascorbate in cancer therapy. Redox Biol. 2016;10:274–84. https://doi.org/10.1016/j.redox.2016.10.010.
33. Verrax J, Calderon PB. Pharmacologic concentrations of ascorbate are achieved by parenteral administration and exhibit antitumoral effects. Free Radic Biol Med. 2009;47(1):32–40. https://doi.org/10.1016/j.freeradbiomed.2009.02.016.
34. Herst PM, Broadley KWR, Harper JL, et al. 1, Pharmacological concentrations of ascorbate radiosensitize glioblastoma multiforme primary cells by increasing oxidative DNA damage and inhibiting G2/M arrest. Free Radic Biol Med. 2012;52(8):1486–93. https://doi.org/10.1016/j.freeradbiomed.2012.01.021.

35. Du J, Martin SM, Levine M, et al. 1, Mechanisms of ascorbate-induced cytotoxicity in pancreatic cancer. Clin Cancer Res. 2010;16(2):509–20. https://doi.org/10.1158/1078-0432.CCR-09-1713.
36. El Banna N, Hatem E, Heneman-Masurel A, et al. Redox modifications of cysteine-containing proteins, cell cycle arrest and translation inhibition: involvement in Vitamin C-induced breast cancer cell death. Redox Biol. 2019;26: 101290. https://doi.org/10.1016/j.redox.2019.101290.
37. Mir HA, Ali R, Wani ZA, et al. 1, Pro-oxidant vitamin C mechanistically exploits p66Shc/Rac1 GTPase pathway in inducing cytotoxicity. Int J Biol Macromol. 2022;205:154–68. https://doi.org/10.1016/j.ijbiomac.2022.02.046.
38. Codini M, Fiorani F, Mandarano M, et al. Sphingomyelin metabolism modifies luminal A breast cancer cell line under a high dose of Vitamin C. Int J Mol Sci. 2023. https://doi.org/10.3390/ijms242417263.
39. Buranasudja V, Doskey CM, Gibson AR, et al. Pharmacologic ascorbate primes pancreatic cancer cells for death by rewiring cellular energetics and inducing DNA damage. Mol Cancer Res. 2019;17(10):2102–14. https://doi.org/10.1158/1541-7786.MCR-19-0381.
40. Lu Y-X, Wu Q-N, Chen D-L, et al. Pharmacological ascorbate suppresses growth of gastric cancer cells with GLUT1 overexpression and enhances the efficacy of oxaliplatin through redox modulation. Theranostics. 2018;8(5):1312–26. https://doi.org/10.7150/thno.21745.
41. Zhou J, Chen C, Chen X, et al. Vitamin C promotes apoptosis and cell cycle arrest in oral squamous cell carcinoma. Front Oncol. 2020;10:976. https://doi.org/10.3389/fonc.2020.00976.
42. Ma Y, Chapman J, Levine M, et al. High-dose parenteral ascorbate enhanced chemosensitivity of ovarian cancer and reduced toxicity of chemotherapy. Sci Transl Med. 2014;6(222):222ra18. https://doi.org/10.1126/scitranslmed.3007154.
43. Lv H, Wang C, Fang T, et al. Vitamin C preferentially kills cancer stem cells in hepatocellular carcinoma via SVCT-2. NPJ Precis Oncol. 2018;2(1):1. https://doi.org/10.1038/s41698-017-0044-8.
44. Yun J, Mullarky E, Lu C, et al. 1, Vitamin C selectively kills KRAS and BRAF mutant colorectal cancer cells by targeting GAPDH. Science. 2015;350(6266):1391–6. https://doi.org/10.1126/science.aaa5004.
45. Deubzer B, Mayer F, Kuçi Z, et al. 1, H2O2-mediated cytotoxicity of pharmacologic ascorbate concentrations to neuroblastoma cells: potential role of lactate and ferritin. Cell Physiol Biochem. 2010;25(6):767–74. https://doi.org/10.1159/000315098.
46. Wu CW, Liu HC, Yu YL, et al. Combined treatment with vitamin C and methotrexate inhibits triple-negative breast cancer cell growth by increasing H2O2 accumulation and activating caspase-3 and p38 pathways. Oncol Rep. 2017;37(4):2177–84. https://doi.org/10.3892/or.2017.5439.
47. Graczyk-Jarzynka A, Goral A, Muchowicz A, et al. Inhibition of thioredoxin-dependent H2O2 removal sensitizes malignant B-cells to pharmacological ascorbate. Redox Biol. 2019;21: 101062. https://doi.org/10.1016/j.redox.2018.11.020.
48. Sant DW, Mustafi S, Gustafson CB, et al. Vitamin C promotes apoptosis in breast cancer cells by increasing TRAIL expression. Sci Rep. 2018;8(1):5306. https://doi.org/10.1038/s41598-018-23714-7.
49. Kim JE, Kang JS, Lee WJ. Vitamin C induces apoptosis in human colon cancer cell line, HCT-8 Via the modulation of calcium influx in endoplasmic reticulum and the dissociation of bad from 14-3-3β. Immune Netw. 2012;12(5):189–95. https://doi.org/10.4110/in.2012.12.5.189.
50. Baek M-W, Cho H-S, Kim S-H, et al. Ascorbic acid induces necrosis in human laryngeal squamous cell carcinoma via ROS, PKC, and calcium signaling. J Cell Physiol. 2017;232(2):417–25. https://doi.org/10.1002/jcp.25438.
51. Wu K, Liu L, Wu Z, et al. Ascorbic acid induces ferroptosis via STAT3/GPX4 signaling in oropharyngeal cancer. Free Radic Res. 2024;58(2):117–29. https://doi.org/10.1080/10715762.2024.2320396.
52. Wang X, Xu S, Zhang L, et al. Vitamin C induces ferroptosis in anaplastic thyroid cancer cells by ferritinophagy activation. Biochem Biophys Res Commun. 2021;551:46–53. https://doi.org/10.1016/j.bbrc.2021.02.126.
53. Vuyyuri SB, Rinkinen J, Worden E, et al. Ascorbic acid and a cytostatic inhibitor of glycolysis synergistically induce apoptosis in non-small cell lung cancer cells. PLoS ONE. 2013;8(6): e67081. https://doi.org/10.1371/journal.pone.0067081.
54. Chen XY, Chen Y, Qu CJ, et al. Vitamin C induces human melanoma A375 cell apoptosis via Bax- and Bcl-2-mediated mitochondrial pathways. Oncol Lett. 2019;18(4):3880–6. https://doi.org/10.3892/ol.2019.10686.

Publisher's Note